Predictive Dynamic Model of Air Separation by Pressure Swing Adsorption

By *Jafar Sadeghzadeh Ahari**, *Saeed Pakseresht*, *Mohammad Mahdyarfar*, *Saeed Shokri*, *Yahya Zamani*, *Ali Nakhaei pour*, and *Fahimeh Naderi*

DOI: 10.1002/ceat.200500226

A general dynamic model is developed for separation of air over a carbon molecular sieve and a zeolite adsorbent for production of nitrogen and oxygen. The proposed model is validated using experimental data from working laboratory scale N_2–PSA and laboratory scale O_2–PSA systems. Simulations studies are performed to investigate the effect of changing various process variables, such as the duration of PSA steps, bed length and feed inlet velocity.

1 Introduction

Traditionally, because of its simplicity and effectiveness, distillation is the most common method by which chemical engineers perform large scale separation tasks. However, the ease of operation and actual cost of distillation depends on the nature of the chemicals, mainly, their relative volatility (α). As α decreases, the thermal efficiency (η), calculated as the ratio of the free energy of mixing to re-boiler heat load at minimum reflux, falls rapidly [1]. Therefore, distillation of chemicals with a low α might require a large number of stages and extensive energy input, both of which would raise the cost of the process.

When distillation becomes too difficult or expensive, chemical engineers often use other methods that are more cost-effective, such as adsorption, membrane separation etc.

Adsorption can be defined as the preferential partitioning of substances from the gaseous or liquid phase on to the surface of solid substrate. In an industrial application, adsorption separation typically involves a column, packed with a suitable adsorbent, through which a fluid stream containing specifically undesired adsorbents is passed in order to achieve separation. This process usually involves fixed bed operations, but moving bed processes also exist. The fixed bed process essentially consists of two steps – the adsorption step and the desorption step. The desorption operation is usually performed either by raising the temperature or by reducing the total pressure. The former characterizes the thermal swing adsorption (TSA) process while the latter is applied in a pressure swing adsorption (PSA).

The pressure swing adsorption (PSA) process, which was originally developed by Skarstrom [2] has become a widely used unit operation for gas separation or purification. PSA is attractive, because it requires no separate desorption steps that need heat input, and because it runs continuously with automatic regeneration of the adsorbent. It is also capable of producing a very pure product [3].

Separation of a gas mixture by PSA is generally accomplished by either using differences in the amount of adsorption at equilibrium condition (equilibrium separation) or by differences in component gas diffusion rates in the sorbent (kinetic separation). One of the uses for the PSA process is nitrogen or oxygen production from air. The process for nitrogen production uses a carbon molecular sieve (CMS), which is kinetically selective for oxygen. In this material, oxygen is the faster diffusing species and is preferentially adsorbed, although at equilibrium, the affinities for oxygen and nitrogen are almost the same.

For oxygen production from air, it is preferable to use a nitrogen selective adsorbent. The common choice being 5A or 13X zeolite, which at ambient temperature exhibits an equilibrium separation factor of about 3.0 in favor of nitrogen.

The application of the PSA process for air separation, requires a dynamic model of the process which can predict the response of product composition and feed consumption, to step changes in process variables such as bed length, flow rate, cycle time, pressure ratio and purge to feed ratio.

Some authors have studied and modeled the PSA system for the oxygen and nitrogen production from air. Raghavan et al. [4] modeled the N_2–PSA system by using a linear driving force (LDF) approximation for intraparticle mass transfer and the linear equilibrium relationship for both oxygen and nitrogen. They also assumed isothermal behavior, negligible pressure drop, axial dispersed plug flow model, linear pressurization and blow down, as well as frozen loading for all pressure changes steps. Hassan et al. [5] modeled the N_2–PSA system by using the Langmuir equilibrium relationships for both oxygen and nitrogen. This is the main difference between two previously mentioned models. Farooq et al. [6] and Shin et al. [7, 8] have considered the pore diffusion for intraparticle mass transfer instead of LDF, which is the most important difference from the Raghavan model [4].

Few authors have studied and modeled the oxygen–PSA system. Fernandez and Kenney [9] have proposed two equi-

[*] J. Sadeghzadeh Ahari (author to whom correspondence should be addressed, sadeghzadehj@ripi.ir), S. Pakseresht, S. Shokri, F. Naderi, Engineering Process Division, Research Institute of Petroleum Industry (RIPI), Tehran 18745 – 4163, Iran; M. Mahdyarfar, Y. Zamani, A. Nakhaei pour, Gas Research Division, Research Institute of Petroleum Industry (RIPI), Tehran 18745 – 4163, Iran.

librium models, one using linear isotherms for each component with another using a linear isotherm for oxygen and a Langmuir isotherm for nitrogen. Farooq et al. [10] and Ruthven and Farooq [11] modeled the experimental system using a linear driving force (LDF) approximation for intraparticle mass transfer and a bicomponent Langmuir isotherm. They also assumed isothermal behavior, negligible pressure drop, linear pressurization and blow down, and axial dispersed plug flow [12].

Ignoring adsorption/desorption during pressurization and depressurization steps through assumption of frozen solid phase may be erroneous, so in the present article a general model for the PSA system is proposed by considering sorption during varied pressure steps. In this work, the mass transfer equations during the pressurization and blow down is considered, with a nonlinear relationship for pressure during these varied pressure steps. Thus in comparison with previous models, such as that of Hassan et al. [6] which is a frozen model for N_2-PSA, and Farooq et al. [10] using a linear relationship for pressure by changing pressure steps for O_2–PSA, the current work includes some modifications and expects to improve the model predictions for both N_2 and O_2 PSA results.

In order to check the predictions of the general model, experimental data from the current authors' laboratory scale two bed PSA unit (for N_2 production from air) and experimental data from the studies of Farooq et al. [10] (for O_2 production from air), have been used.

2 Theory

2.1 Process Description

The process consider here utilizes two identical columns packed with adsorbent. These are connected and operated in a four step cycle as shown in Fig. 1

During step 1, feed is supplied at to bed 1, where adsorption of the faster diffusing or higher affinity component occurs. The other component is removed as a relatively pure product. A portion of this product is throttled to for purging in bed 2. In step 2, bed 1 undergoes blow down through the feed end, and bed 2 is pressurized with feed. This cycle is repeated in steps 3 and 4 except that the points of feed introduction, purge, and blow down are reversed with respect to beds 1 and 2. Fig. 2 shows the pressure changes in bed 1 during one cycle time.

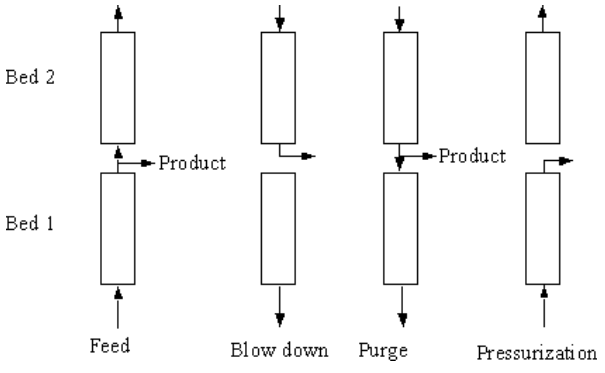

Figure 1. Step involved in the PSA Cycle.

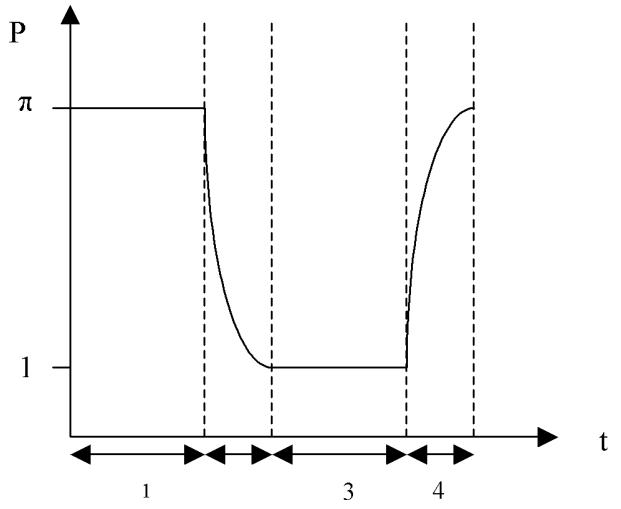

Figure 2. Pressure changes during one cycle of the PSA system.

A number of minor modifications of this cycle are possible. One that is considered here is pressurization with product rather than feed. Also, a variety of conditions may be used, giving rise to terminology such as vacuum swing adsorption.

2.2 Experimental Setup

The apparatus used, as illustrated in Fig. 3, consisted of two stainless steel columns of 1.0 m in length and 0.025 m in ID, which were filled with carbon molecular sieves (CMS). The columns can be operated either separately or together, depending on the PSA cycle being studied.

An electronic timer, which actuates 8 solenoid valves, is located at the inlet/outlets of the column together with pressure, temperature and flow indicators.

In the pressurization step of the column A, the entrance solenoid valve to this column is opened and the outlet valves are closed. The final pressure of the column could be controlled by a backpressure valve and actually could be increased to 10 barg depend on the experimental condition. Meanwhile at the column A pressurization step, the column B is in the blow down step. After pressurization of column A, the outlet solenoid valves were opened and the product was produced. A portion of this product was used to purge the column B by a separate line and the purge flow rate was controlled by a mass flow controller. After the adsorption and production step with column A, the function of columns A and B was changed. The third step consisted of column A blow down (by opening of the outlet solenoid valve to the

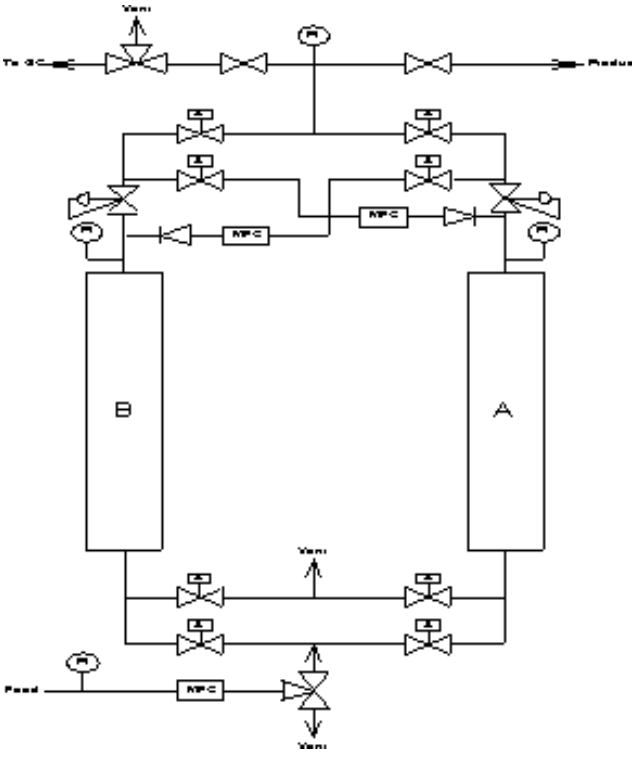

Figure 3. Schematic diagram of the PSA experimental system.

atmosphere and closing the other valves) and pressurization of column B (by closing of the outlet valves). The adsorption and production of column B is performed simultaneously with the purge step of the column A. At the end of this step, one cycle of PSA system is completed.

A fraction of a bed product during the adsorption step was collected in a proper sampling vessel and analyzed with a Shimadzu PTF 4C gas chromatograph with a 2 m long and 3 mm diameter 5A molecular sieve column and TCD detector. The range of the accuracy of measurement was ± 0.1 mol.-%.

2.3 Mathematical Model

In order to develop a mathematical model for this system the following assumptions are introduced:

1. The system is considered isothermal with total pressure remaining constant through the bed during high pressure and low pressure flow operations.
2. The equilibrium relationship is nonlinear and described by a Langmuir isotherm.
3. Plug flow prevails in the bed with axial dispersion.
4. The mass transfer rate is represented by a linear driving force (LDF) expression.
5. The pressure drop through the adsorbent bed is negligible.
6. The fluid velocity within the bed during adsorption and desorption varies along the length of the column, as determined by the mass balance.
7. The ideal gas law applies.
8. During pressurization and blow down, the total pressure in the bed changes non-linearly with time and the adsorption/desorption occurs.

Subject to these assumptions, the dynamic behavior of the system may be described by the following set of equations for each bed[1)].

Step 1: High pressure adsorption in bed 2 (purge step in bed 1):

a) Material balance in gas phase:

$$\frac{\partial C_{A2}}{\partial t} - D_{L2}\frac{\partial^2 C_{A2}}{\partial z^2} + V_2\frac{\partial C_{A2}}{\partial z} + C_{A2}\frac{\partial V_2}{\partial z} + \left(\frac{1-\breve{\alpha}}{\breve{\alpha}}\right)\frac{\partial q_{A2}}{\partial t} = 0 \tag{1}$$

$$\frac{\partial C_{B2}}{\partial t} - D_{L2}\frac{\partial^2 C_{B2}}{\partial z^2} + V_2\frac{\partial C_{B2}}{\partial z} + C_{B2}\frac{\partial V_2}{\partial z} + \left(\frac{1-\breve{\alpha}}{\breve{\alpha}}\right)\frac{\partial q_{B2}}{\partial t} = 0 \tag{2}$$

b) Continuity:

$$C_{A2} + C_{B2} = C_t = C_{HP}\ (\text{Constant}) \tag{3}$$

c) Overall material balance:

$$C_{HP}\frac{\partial V_2}{\partial z} + \frac{1-\breve{\alpha}}{\breve{\alpha}}\left(\frac{\partial q_{A2}}{\partial t} + \frac{\partial q_{B2}}{\partial t}\right) = 0 \tag{4}$$

d) Mass transfer rates:

$$\frac{\partial q_{A2}}{\partial t} = k_{A2}(q^*_{A2} - q_{A2}) \qquad \frac{\partial q_{B2}}{\partial t} = k_{B2}(q^*_{B2} - q_{B2}) \tag{5}$$

e) Adsorption equilibrium:

$$\frac{q^*_{A2}}{q_{As}} = \frac{b_A C_{A2}}{1 + b_A C_{A2} + b_B C_{B2}} \qquad \frac{q^*_{B2}}{q_{Bs}} = \frac{b_B C_{B2}}{1 + b_A C_{A2} + b_B C_{B2}} \tag{6}$$

f) Boundary conditions:

$$D_L\frac{\partial C_{A2}}{\partial z}|_{z=0} = -V_{0H}(C_{A2}|_{z=0^-} - C_{A2}|_{z=0}) \tag{7}$$

$$\frac{\partial C_{A2}}{\partial z}|_{z=L} = 0 \tag{8}$$

$$\frac{\partial V_2}{\partial z}|_{z=L} = 0 \tag{9}$$

1) List of symbols at the end of the paper.

$$V_2|_{z=0} = V_{0H} \tag{10}$$

Step 2: Blow down of bed 2 (Pressurization in bed 1):

In this step, the total concentration varies with time, such that, except for the following, the other equations remain unchanged:

$$C_{A2} + C_{B2} = C_2 = f(t) \tag{11}$$

The overall material balance is given by:

$$C_2 \frac{\partial V_2}{\partial z} + \frac{\partial C_2}{\partial t} + \left(\frac{1-\check{\alpha}}{\check{\alpha}}\right)\left(\frac{\partial q_{A2}}{\partial t} + \frac{\partial q_{B2}}{\partial t}\right) = 0 \tag{12}$$

The following are the boundary conditions:

$$D_{L2} \frac{\partial C_{A2}}{\partial z}|_{z=0} = 0 \tag{13}$$

$$\frac{\partial C_{A2}}{\partial z}|_{z=L} = 0 \tag{14}$$

$$V_2|_{z=L} = 0 \tag{15}$$

$$\frac{\partial V_2}{\partial z}|_{z=0} = 0 \tag{16}$$

Step 3: Purge of bed 2 (adsorption in bed 1):

The equations for step 1 also remain unchanged in step 3 with the following changes in boundary conditions:

$$D_{L2} \frac{\partial C_{A2}}{\partial z}|_{z=0} = -V_{OL}(C_{A2}|_{z=0^-} - C_{A2}|_{z=0}) \tag{17}$$

$$C_{A1}|_{z=L} = \left(\frac{P_L}{P_H}\right) C_{A2}|_{z=L} \tag{18}$$

$$\frac{\partial V_2}{\partial z}|_{z=0} = 0 \tag{19}$$

$$V_2|_{z=L} = V_{0L} \tag{20}$$

Step 4: Pressurization of bed 2 (Blow down in bed 1):

With the following changes in boundary conditions, the equations of step 2 can be used for step 4:

$$D_L \frac{\partial C_{A2}}{\partial z}|_{z=0} = -V_{0H}(C_{A2}|_{z=0^-} - C_{A2}|_{z=0}) \tag{21}$$

$$\frac{\partial C_{A2}}{\partial z}|_{z=L} = 0 \tag{22}$$

$$V_2|_{z=L} = 0 \tag{23}$$

$$\frac{\partial V_2}{\partial z}|_{z=0} = 0 \tag{24}$$

The valid initial conditions for the start up of the cyclic operation with two clean beds are the following sets of equations:

$$C_{A2}(z,0) = 0 \qquad C_{B2}(z,0) = 0$$

$$q_{A2}(z,0) = 0 \qquad q_{B2}(z,0) = 0$$

$$C_{A1}(z,0) = 0 \qquad C_{B1}(z,0) = 0$$

$$q_{A1}(z,0) = 0 \qquad q_{B1}(z,0) = 0 \tag{25}$$

2.4 Solution Technique

In order to solve the above set of second and first order coupled partial differential equations, they need to be dimensionalized and discretized in space using the orthogonal collocation method. The set of equations contains 2m unknowns, m–1 mole fractions in the bulk stream (dimensionless form of concentration in gas phase), m adsorbed phase concentrations in the adsorbent, and the flow velocity of the stream in the column.

The resulting linear equations (the overall material balance upon discrimination, yielded a set of algebraic equations) and ordinary differential equations were solved by LU decomposition and Runge-Kutta order 4 (for the nitrogen–PSA system) or Gear methods (for the oxygen-PSA system).

For the N_2–PSA system, a visual basic code in double precision format, and for the O_2–PSA system, a Matlab code were developed to solve the set of coupled differential-algebraic equations. Fig. 4 shows the flow chart used in this study.

3 Results and Discussion

3.1 N_2–PSA System

The parameters used in simulating the experimental runs for N_2–PSA system are summarized in Tab. 1. The predictions of the theoretical model have been compared with the experimental results. The experimental and model results in the adsorption step are shown in Fig. 5.

According to Fig. 5 a good agreement between the experiments and the simulation is observed.

In order to gain a better understanding of the N_2–PSA process, the effect of process variables on the nitrogen purity obtained by simulation studies is studied.

Effect of Duration of Feed, Blow Down and Pressurization Steps

The effect of duration of high pressure feed step is shown in Fig. 6. An increase in duration, results in greater oxygen

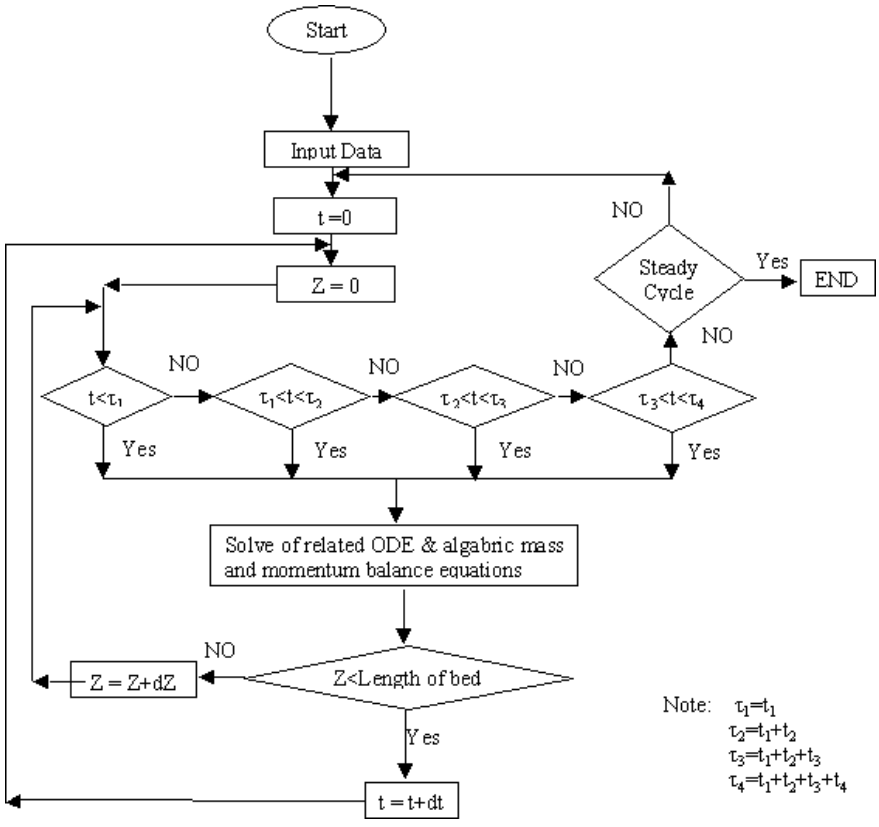

Figure 4. Flow chart of the PSA simulator.

Table 1. Used parameters in simulation of $N_{2-PSA\ system}$.

Feed composition	21.8 % Oxygen, 78.2 % Nitrogen
Adsorbent	CMS
L (m)	1.0
r_i (m)	0.0125
e	0.4
T_0 (°C)	30.0
Blow down pressure (atm)	1.0 atm
Pressurization pressure (atm)	8.0
Axial dispersion coefficient (m^2/s)	$4.876 \cdot 10^{-4}$
Equilibrium constant for oxygen (K_A)	9.25
Equilibrium constant for nitrogen (K_B)	8.9
LDF constant for oxygen (k_A) (s^{-1})	$44.71 \cdot 10^{-3}$
LDF constant for nitrogen (k_B) (s^{-1})	$7.62 \cdot 10^{-3}$
Saturation constant for oxygen (q_{AS}) (mol/m^3)	$2.64 \cdot 10^3$
Saturation constant for nitrogen (q_{BS}) (mol/m^3)	$2.64 \cdot 10^3$

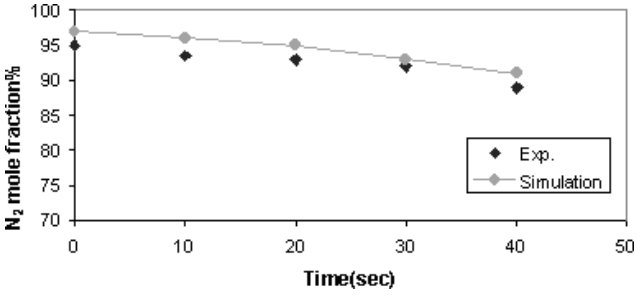

Figure 5. Comparison of simulation and experimental product purity results at the high pressure (adsorption) step as a function of adsorption time.

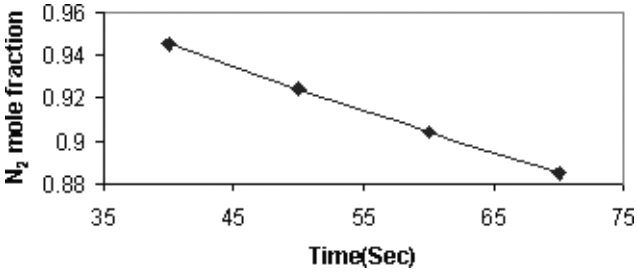

Figure 6. Effect of duration of step time on the N_2–PSA system. t_2 = 10 sec, t_3 = 40 sec, t_4 = 10 sec, bed length = 1.0 m, V_L = 0.1 m/sec, V_H = 0.16 m/sec, P_H = 8.0 atm, P_L = 1.0 atm.

contamination for the product, but increasing quantities of product.

Since the adsorbed impurity, oxygen diffuses out of the adsorbent during the blow down step, a longer blow down time results in a cleaner bed. The effect of blow down time on product purity is given in Tab. 2. According to Tab. 2 it is seen that the blow down time has a good effect on the product purity.

Table 2. Effect of duration of blow down step on N_2–PSA system.

t_2 (sec)	Y (N_2)
10	0.9455
15	0.9485
20	0.9511
25	0.9534
$t_1 = t_3 = 40$ sec, $t_4 = 10$ sec, bed length = 1.0 m $V_1 = 0.1$ m/sec, $V_H = 0.16$ m/sec, $P_H = 8.0$ atm, $P_L = 1.0$ atm	

The results for various times for the pressurization step at cyclic steady state are given in Fig. 7. The results show that as the duration increases, the purity decreases.

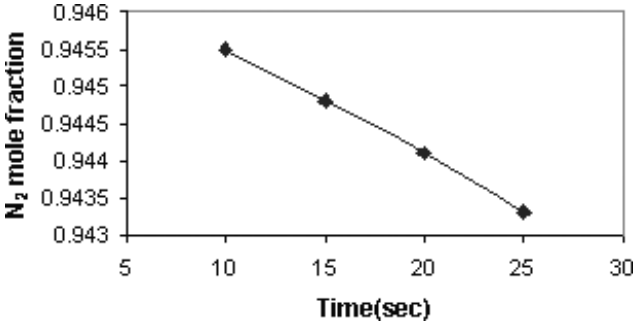

Figure 7. Effect of duration of the pressurization step on the N_2–PSA system. $t_1 = 40$ sec, $t_2 = 10$ sec, $t_3 = 40$ sec, bed length = 1.0 m, $V_L = 0.1$ m/sec, $V_H = 0.16$ m/sec, $P_H = 8.0$ atm, $P_L = 1.0$ atm.

Effect of Inlet Velocity

The inlet velocity is directly related to the purity of product, and this effect is shown in Fig. 8.

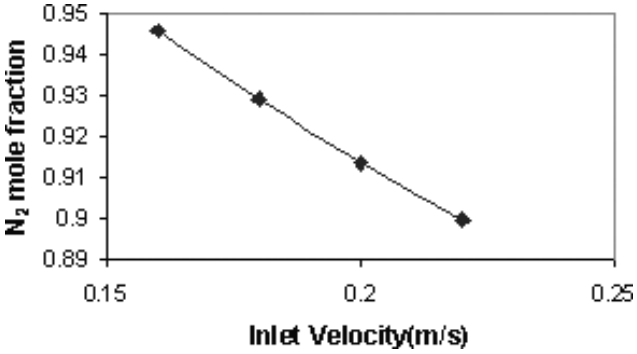

Figure 8. Effect of inlet velocity on the N_2–PSA system. Cycle time = 100 sec, t_1, $t_3 = 0.4 \cdot$ cycle time, t_2, $t_4 = 0.1 \cdot$ cycle time, bed length = 1.0 m, $V_L = 0.1$ m/sec, $P_H = 8.0$ atm, $P_L = 1.0$ atm.

Effect of Bed Length

The effect of varying the bed length is illustrated in Fig. 9. This shows that with a longer bed, higher purity of product is acquired.

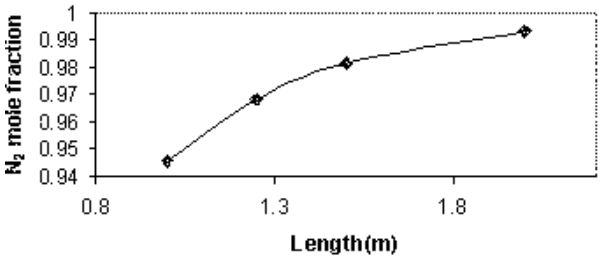

Figure 9. Effect of bed length on the N_2–PSA system. Cycle time = 100 sec, t_1, $t_3 = 0.4 \cdot$ cycle time, t_2, $t_4 = 0.1 \cdot$ cycle time, $V_H = 0.16$ m/sec, $V_L = 0.1$ m/sec, $P_H = 8.0$ atm, $P_L = 1.0$ atm.

Cycle Time

The effect of cycle time on the product purity is shown in Tab. 3. It is seen that the product purity increases when cycle time decreases.

Table 3. Effect of cycle time on N_2–PSA system.

Cycle time (sec)	Y (N_2)
50	0.951
100	0.9455
150	0.9251
200	0.8965
250	0.8659
300	0.8416
$t_1, t_3 = 0.4 \cdot$ cycle time, $t_2, t_4 = 0.1 \cdot$ cycle time, bed length = 1.0 m $V_H = 0.16$ m/sec, $V_1 = 0.1$ m/sec, $P_H = 8.0$ atm, $P_L = 1.0$ atm	

3.2 O_2–PSA System

The parameters used in simulating the Farooq et al. [10] experimental runs for the O_2-PSA system are summarized in Tab. 4.

3.2.1 Model Validation

The experimental results, together with the theoretically predicted values from this work and also the Farooq simulation, are summarized in Figs. 10–13.

Fig. 10 shows that with increasing adsorption pressure, the purity of the product will increase due to the extra nitrogen adsorption on the adsorbent.

In Fig. 11 it is seen that with increasing adsorption step pressure, the recovery of oxygen decreases due to the extra oxygen adsorption at higher pressure. The simulation results (Farooq et al. and this work) agree well with the experimental results.

Figs. 12 and 13 show that under the condition of the experiments, oxygen recovery increases continuously with increasing product rate and there is very little change in

Table 4. Parameters used in simulation of O_2–PSA system.

Feed composition	21 % O_2, 79 %N_2
Adsorbent	Linde 5A zeolite
L (m)	0.35
r_i (m)	0.0175
d_p (m)	0.000707
e	0.40
T_0 (°C)	25.0
Blow down pressure (atm)	1.0
Purge pressure (atm)	1.07
Peclet number	500.0
Duration of step 1 or 3	0.2 of total cycle time
Duration of step 2 or 4	0.3 of total cycle time
Equilibrium constant for oxygen (K_A)	4.7
Equilibrium constant for nitrogen (K_B)	14.8
LDF constant for oxygen (k_A) (s^{-1})	62.0 (at 1 atm)
LDF constant for nitrogen (k_B) (s^{-1})	19.7 (at 1 atm)
Saturation constant for oxygen (q_{AS})(mol/m^3)	$5.26 \cdot 10^3$
Saturation constant for nitrogen (q_{BS}) (mol/m^3)	$5.26 \cdot 10^3$

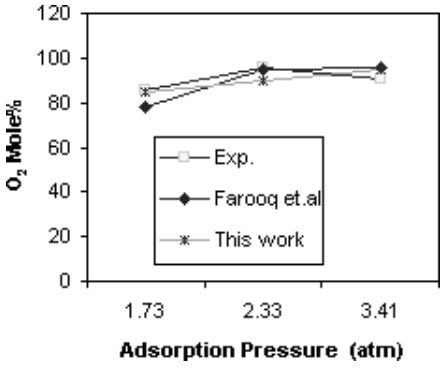

Figure 10. Comparison of product purity vs. adsorption pressure between current work and simulation results of Farooq et al.

product purity. Presumably at higher product withdrawal rates, the purity will eventually decline. These figures demonstrate a very good agreement between the experimental and the two systems modelled (the scale of the oxygen purity axis is magnified in Fig. 12).

3.2.2 Specific Comparisons

The effects of varying the inlet velocity, duration of feed, bed length and cycle time were investigated and the results are summarized in Figs. 14–19. As can be seen from Fig. 14, with increasing velocity, even with constant flow rate, the purity of product will gradually decrease.

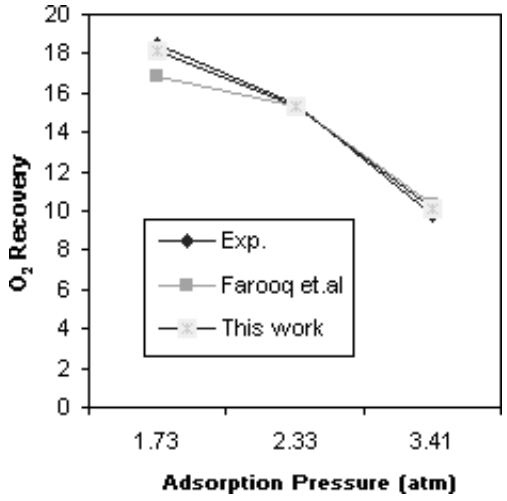

Figure 11. Comparison of product recovery vs. adsorption pressure between current work and simulation results of Farooq et al.

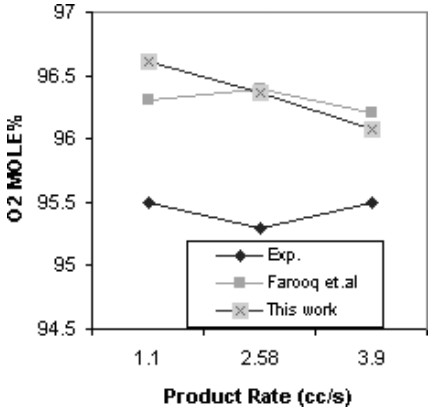

Figure 12. Comparison of product purity vs. product rate between current work and simulation results of Farooq et al.

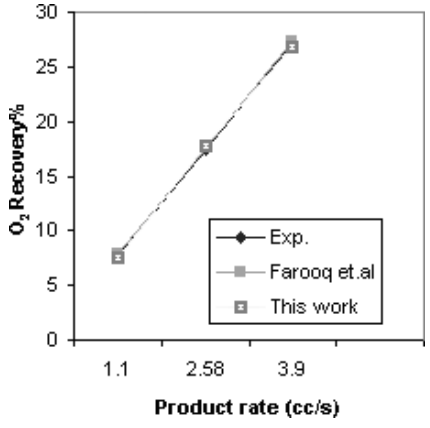

Figure 13. Comparison of product recovery vs. product rate between current work and simulation results of Farooq et al.

Fig. 15 shows that with increasing time of the adsorption step, the product purity will considerably decrease. Increasing the adsorption time step will cause the saturation of the adsorbent combined with passing of the breakthrough curve

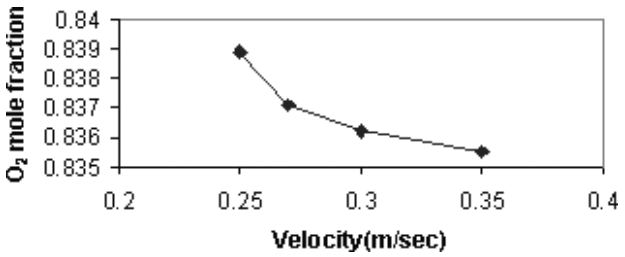

Figure 14. Effect of inlet velocity on the O_2–PSA system. Cycle time = 150 sec, t_1, t_3 = 0.2 · cycle time, t_2, t_4 = 0.3 · cycle time, bed length = 0.35 m, product flow rate = $1.13 \cdot 10^{-6}$ m^3/sec, P_H = 1.66 atm, P_L = 1.0 atm.

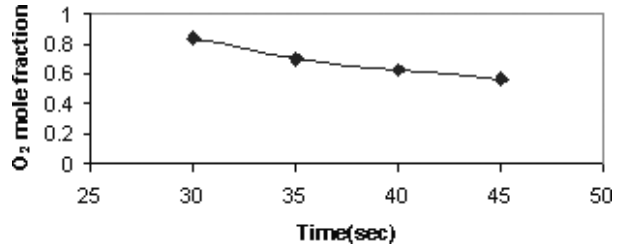

Figure 15. Effect of duration of high pressure step on the O_2–PSA system. t_2 = 45 sec, t_3 = 30 sec, t_4 = 45 sec, bed length = 0.35 m, product flow rate = $1.13 \cdot 10^{-6}$ m^3/sec, V_H = 0.35 m/sec, P_H = 1.66 atm, P_L = 1.0 atm.

from the end of the adsorption bed and finally decreases the purity of product.

In Fig. 16, the trend of increasing the oxygen purity versus increasing bed length is plotted.

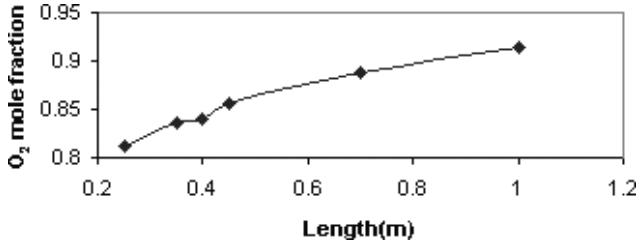

Figure 16. Effect of bed length on the O_2–PSA system. Cycle time = 150 sec, t_1, t_3 = 0.2 · cycle time, t_2, t_4 = 0.3 · cycle time, V_H = 0.35 m/sec, product flow rate = $1.13 \cdot 10^{-6}$ m^3/sec, P_H = 1.66 atm, P_L = 1.0 atm.

Fig. 17 shows the effect of blow down step time to the product purity. When the time of this step is increased, the adsorption beds have enough time to release more adsorbed nitrogen, so that in the production step, the bed will produce more purified oxygen.

Figs. 18 and 19 show the effect of pressurization time and cycle time on product purity. It is seen that with increasing the time of this step and cycle time, the purity of the product decreases due to the saturation of the bed and passing nitrogen breakthrough from the bed end.

4 Conclusions

In this work a general dynamic model was developed with modification of the pressure changes relationship of Farooq et al. [10] model, which was previously developed for an equilibrium, controlled oxygen-PSA system.

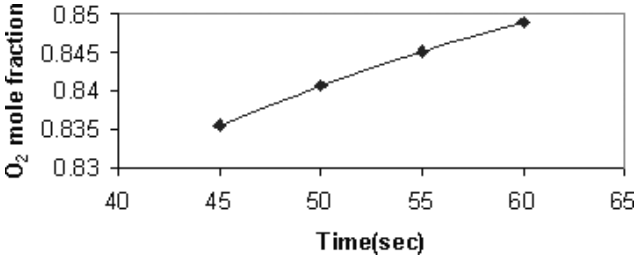

Figure 17. Effect of duration of blow down step on the O_2–PSA system. t_1 = 30 sec, t_3 = 30 sec, t_4 = 45 sec, bed length = 0.35 m, product flow rate = $1.13 \cdot 10^{-6}$ m^3/sec, V_H = 0.35 m/sec, P_H = 1.66 atm, P_L = 1.0 atm.

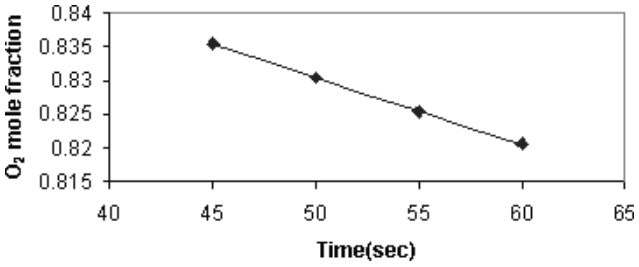

Figure 18. Effect of duration of pressurization step on the O_2–PSA system. t_1 = 30 sec, t_2 = 45 sec, t_3 = 30 sec, bed length = 0.35 m, product flow rate = $1.13 \cdot 10^{-6}$ m^3/sec, V_H = 0.35 m/sec, P_H = 1.66 atm, P_L = 1.0 atm.

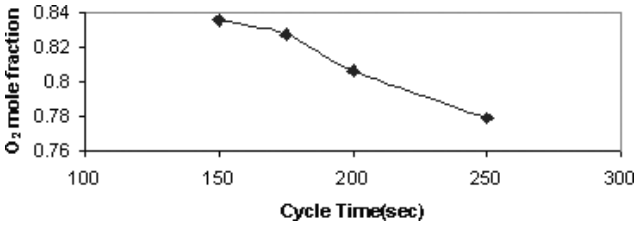

Figure 19. Effect of cycle time on the O_2–PSA system. Bed length = 0.35 m, t_1, t_3 = 0.3 · cycle time, t_2, t_4 = 0.4 · cycle time, V_H = 0.35 m/sec, product flow rate = $1.13 \cdot 10^{-6}$ m^3/sec, P_H = 1.66 atm, P_L = 1.0 atm.

The developed model was applied to the N_2–PSA and O_2–PSA systems and a good agreement between the experimental and simulation results are observed. The effects of the duration of the PSA steps, cycle time, inlet feed velocity and bed length on product purity is also studied. The results show that the product (O_2 and N_2) purity increases when the duration of the blow down step or bed length increases. However, with increase of other process variables such as cycle time, inlet velocity, duration of the step and duration of pressurization step, product purity will be decreased.

The cycle used here is the simple two bed Skarstrom cycle but there is no reason preventing the application of the same model to more complex multi-bed systems, which are commonly used in large scale units.

Received: June 26, 2005 [CET 0226]

Symbols used

b_A,b_B	[m^3/mole]	langmuir constant for component A and B
C_{A2}, C_{B2}	[mole/m^3]	concentration of components A and B in gas phase in bed 2
C_2	[mole/m^3]	total gas phase concentration at blow down step
C_H	[mole/m^3]	total gas phase concentration at high- pressure step
d_P	[m]	particle diameter
D_L	[m^2/s]	axial dispersion coefficient
k_A,k_B	[s^{-1}]	effective mass transfer coefficient for components of A and B
K_A, K_B	[–]	adsorption equilibrium constant for components A and B
L	[m]	bed length
P_H, P_L	[atm]	column pressure at high-pressure step and low-pressure step
q_{A1}, q_{A2}, q_{B1}, q_{B2}	[mole/m^3]	concentration of components of A and B in solid phase in bed 1 and bed 2
q_{AS}, q_{BS}	[mol/m^3]	saturation constants for component A and B
q^*_{A1}, q^*_{A2}	[mole/m^3]	value of q_{A1},and q_{A2} in equilibrium with C_{A1} and C_{A2}
q^*_{B1}, q^*_{B2}	[mole/m^3]	value of q_{B1},and q_{B2} in equilibrium with C_{B1} and C_{B2}
r_i	[m]	inner diameter of column
t_1	[s]	duration of high-pressure step
t_2	[s]	duration of blow down step
t_3	[s]	duration of purge step
t_4	[s]	duration of pressurization step
T_0	[°C]	ambient temperature
V_2	[m/s]	velocity in bed 2
V_{0H}, V_{0L}	[m/s]	inlet velocity during high-pressure step and purge step
z	[m]	axial distance from column inlet
ε	[–]	bed Voidage

References

[1] D. M. Ruthven, *Principles of Adsorption and Adsorption Process*, Wiley, NewYork **1984**.
[2] C. W. Skartrom, *Ann. N. Y. Acad. Sci.* **1959**, *72 (13)*, 751.
[3] X. Lu, R. Mady, D. Rothestein, M. Jaronice, *Chem. Eng. Sci.* **1990**, *45*, 1097.
[4] N. S. Raghavan, D. M. Ruthven, *AIChE J.* **1985**, *31*, 2017.
[5] M. M. Hassan, D. M. Ruthven, N. S. Raghavan, *Chem. Eng. Sci.* **1986**, *41 (5)*, 1333.
[6] S. Farooq, D. M. Ruthven, *Chem. Eng. Sci.* **1990**, *45*, 107.
[7] H. S. Shin, K. S. Knaeble, *AIChE J.* **1987**, *33*, 654.
[8] H. S. Shin, K. S. Knaeble, *AIChE J.* **1988**, *34*, 1409.
[9] G. Fernandez, C. Kenney, *Chem. Eng. Sci.* **1983**, *38*, 827.
[10] S. Farooq, D. M. Ruthven, H. A. Boniface, *Chem. Eng. Sci.* **1989**, *44*, 2809.
[11] D. M. Ruthven, S. Farooq, *Gas Sep. Purif.* **1990**, *41*, 141.
[12] A. M. M. Mendes, A. V. Carlos, A. E. Rodrigues, *Sep. Purif. Technol.* **2001**, *24*, 173.

